Tests to Establish Flow Distortion Criteria for Lift Engines

B. I. Tyson*
Douglas Aircraft Company, Long Beach, Calif.

A test program was conducted to investigate performance of lift-engine inlets and to develop a static-test device that would simulate flow distortions at the face of a lift engine. Wind-tunnel tests indicated that the combination of high forward speed and low engine power would cause flow separation and excessive distortion. A scoop inlet was developed that enabled the flow to turn without separation. For improved pressure recovery in static and near-static operation, longitudinal vanes in the scoop were used to augment the inlet area. By opening the vanes at low speed and closing them for engine restart, acceptable inlet performance was obtained. The wind-tunnel data showed that for a given engine-face velocity the pressure losses, both with and without scoops, were in good agreement when compared at the same approach velocity. This led to the development of a static-test distortion generator that simulated the pressure gradients measured in the wind tunnel. The distortion-generator data agree well with the wind-tunnel data, which indicated that the generator technique should be useful for engine development testing.

Nomenclature

C_s = pressure coefficient $(P_{t_0} - P_s)/q_2$
d = diameter, in.
h = depth of engine face, in.
P = pressure, psi
q = dynamic pressure, $\rho V^2/2$
r = radius, in.
V = velocity, fps
α = angle of attack, deg
θ = thrust-axis inclination (Fig. 1) or angular location (Fig. 21), deg
ρ = density, slugs/ft^3
ψ = yaw angle, deg

Subscripts

A = approach
L = local
s = static
T = total
t = tip
0 = freestream
2 = engine-face station

Introduction

THE development of a jet engine is usually well advanced before any information about the aircraft installation is made available to the engine manufacturer. As a result, the behavior of the engine, when subject to inlet flow distortion, usually remains a mystery until the first flight tests. Too often the results of flight tests indicate that costly modifications of the air-induction system or engine are required in order to eliminate problems of engine compressor stall. A solution of this problem is to test the prototype inlet-engine installation before the airplane design is "frozen." Distortion testing is especially attractive for a lift engine because a simple test at sea level is descriptive of performance at the operational altitude.

A series of wind-tunnel tests was therefore conducted in order to provide information about lift-engine inlet design and performance (see Ref. 1). The measured flow distortions at the simulated engine face were then used to develop a static-test device that would simulate the in-flight distortions. Subsequent tests of this device with the prototype lift engine can be used to evaluate the distortion tolerance of the engine and estimate in-flight behavior. A summary of the inlet pressure losses and flow distortions measured during the wind-tunnel tests and the development of the distortion-generator test model are described in this paper.

Presented as Preprint 64-608 at the AIAA Transport Aircraft Design and Operations Meeting, Seattle, Wash., August 10–12, 1964; revision received November 30, 1964. This work was conducted on subcontract to Continental Aviation and Engineering Corporation and is a part of U. S. Air Force Aeronautical Systems Division Project 668A.

* Aerodynamicist, Propulsion-Aerodynamics Group, Aircraft Division. Member AIAA.

Inlet-Design Considerations

Vertically mounted lift-engine installations present a unique problem to the inlet designer: to design an inlet that turns the engine air flow through 90° and yet prevents excessive total- and static-pressure distortion. The problem is further complicated by the compactness of the engine installation that precludes the use of the large-radius elbows recommended in ducting handbooks for efficient flow turning. One method of reducing the frontal area of the engine installation is to use a bellmouth inlet. The bellmouth lip must have a reasonably small radius, in order to permit close spacing of adjacent engines. This introduces the possibility of flow separation and resultant pressure distortion. Even so, the compactness afforded by the bellmouth inlet makes it a logical choice for a lift-engine installation and provides an incentive to find ways of improving its performance.

There are two design points for a lift-engine inlet takeoff and landing. During takeoff, the engine air flow is accelerated around the inlet lips, and the inlet acts as a bellmouth, with little chance of flow separation. Before landing, however, the inlet behaves like a static-pressure orifice until engine starting and acceleration can be accomplished. The starting cycle therefore imposes a more stringent design requirement for minimizing inlet-flow distortion.

Some insight into the inlet-design problem can be gained by examining the forces acting at the inlet. Figure 1 shows a schematic diagram of the inlet flow. The force required to turn the inlet air flow into the engine is created by pressures acting on the lip surfaces, a low pressure upstream, and a high pressure downstream. The momentum diagram shown was used to compute the magnitude of the resultant lip force as a function of the inlet velocity ratio V_0/V_2 and the thrust-axis inclination angle θ. The results are presented in Fig. 2. Note that the force required increases as the flight speed is increased and decreases as the engine is inclined forward into the air stream. Since high peak pressures on the lip surface

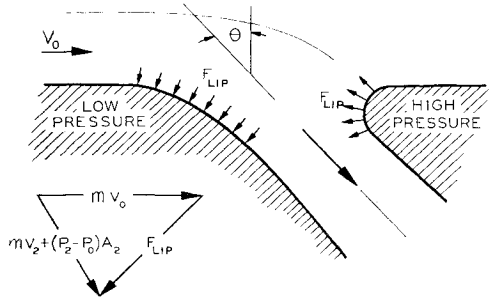

Fig. 1 Schematic diagram of inlet flow.

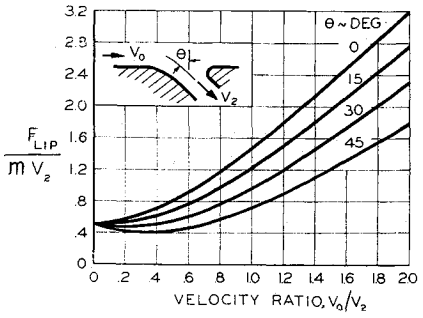

Fig. 2 Calculated lip force.

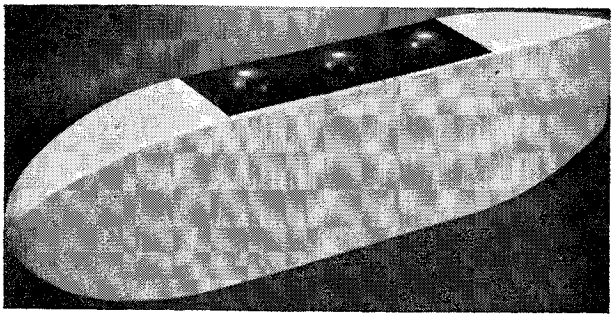

Fig. 3 Pod test model.

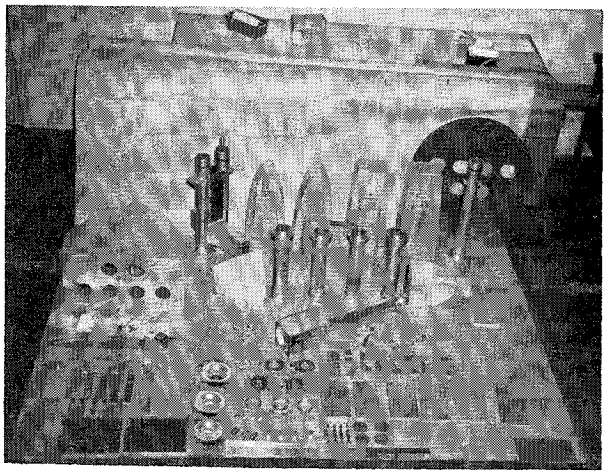

Fig. 4 Model components.

are required to develop the lip force, the possibility of flow separation is greatest at the high velocity ratios. The results also indicate that engine inclination is not a practical method of improving inlet performance because of the large angles required to make significant reductions in lip force. Furthermore, even if large angles could be tolerated, it is doubtful that sufficient ram pressure could be supplied to air-start the engines.

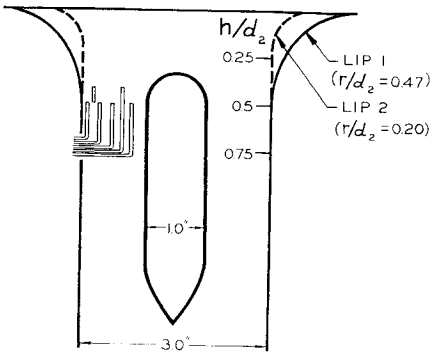

Fig. 5 Typical engine module.

Inlet Test Program

An extensive wind-tunnel test program was conducted to obtain inlet data for clustered lift-engine arrangements over a range of angles of attack and yaw. The test models simulated both fuselage and podded-engine installations with either in-line or side-by-side engine arrangements. Since the data for all of these configurations were similar, the discussion of results can be confined to one configuration. The configuration chosen is the three-engine, in-line pod shown in Fig. 3. The effects of angle of attack and yaw on pressure loss have been reported in Ref. 1.

Inlet Model

The pod model was composed of three engine modules in line, each containing engine-face instrumentation, a butterfly valve for regulating the flow rate, and an orifice plate to meter the flow. Nose and tail cones were added to the modules to complete the pod assembly. Figure 4 shows the model components. Note the plenum chamber used to connect the model with the suction system.

The dimensions of a typical engine module and a sketch of the two inlet lip shapes tested are shown in Fig. 5. The lip radii are fairly large in order to provide an efficient bellmouth entry at static conditions. Also shown in Fig. 5 are the instrumentation locations used to measure pressures at the simulated engine-face stations. The pressure instrumentation consisted of 8 rakes, 45° apart, each with 4 total-pressure and 2 static-pressure probes.

Inlet Performance

Total-pressure loss is a measure of inlet performance. Whether it is caused by skin friction or flow separation, this loss is proportional to the local dynamic pressure. It is there-

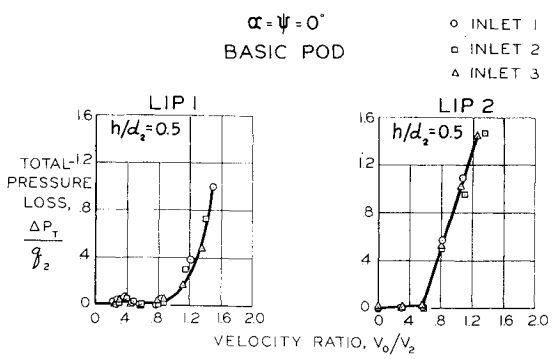

Fig. 6 Basic pod inlet performance.

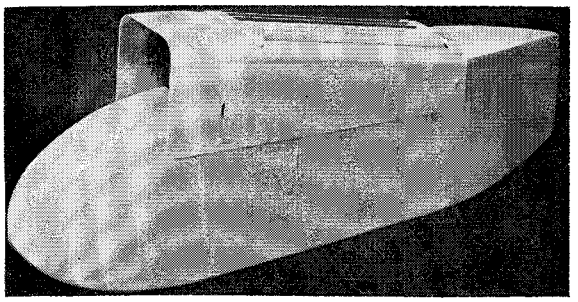

Fig. 7 Revised scoop, auxiliary vanes open.

fore customary to express the measured inlet total-pressure loss as a percent of the dynamic pressure. The reference dynamic pressure q_2 for these tests, taken at the engine-face station, was calculated during the tests by using the measured mass flow, pressure, and temperature.

Pod Pressure Losses

Total-pressure losses for the model are presented in Fig. 6. The rise in pressure loss indicates flow separation, which occurs at a relatively high velocity ratio. This is in accordance with the trends predicted by the earlier analysis of inlet flow. Since such large losses would not permit trouble-free air starts and engine acceleration during landing, improvements in the inlet were sought.

Scoop Inlet

After several configurations were tested, including "flapped" inlets and a configuration with annular vanes at the inlet leading edge, it was decided that the most effective way of improving high-speed performance would be to reduce the velocity ratio at the engine entry. Accordingly, the scoop fairing shown in Fig. 7 was developed to diffuse the entering air flow. The scoop was 5.2 in. high at the leading edge and had vanes along the upper surface to augment the scoop-inlet area during takeoff. In addition, the scoop trailing edge was raised to permit the internal boundary layer to escape without being ingested by the last engine. Performance with vanes open and with vanes closed is shown in Fig. 8. Note the improvement at static conditions because of the vanes. By using a configuration with vanes open during takeoff and vanes closed at high speed, the pressure losses can be held to an acceptably low level over the operating range of the lift engine. In addition, the "ram" effect provided by the scoop should aid in air-starting and improve acceleration response during landing.

Velocity Distortion

The average total-pressure loss of an inlet is indicative of the thrust-loss penalty of the engine installation but is not descriptive of flow distortion. The radial and circumferential

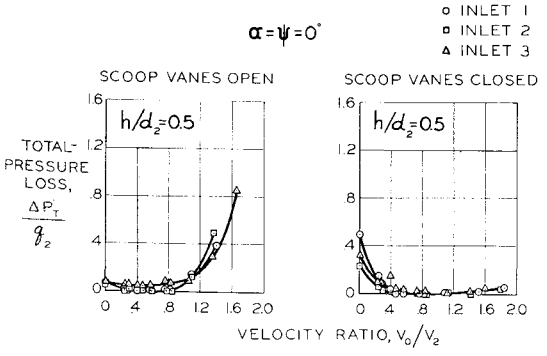

Fig. 8 Effect of scoop vanes on performance, lip 1.

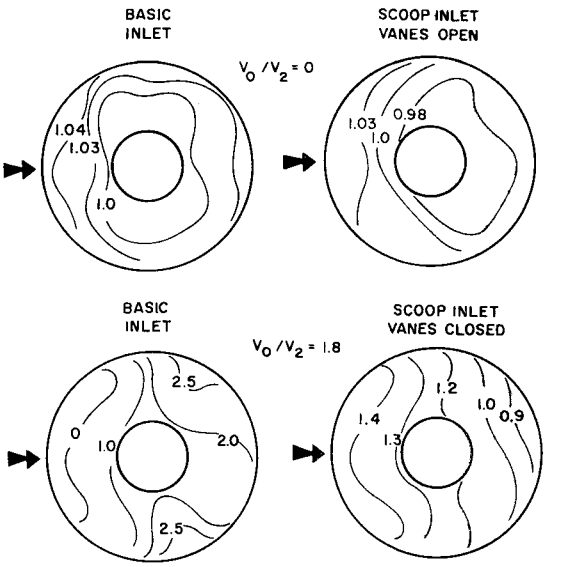

Fig. 9 Inlet distortion comparison; contours are lines of local velocity ratio V_L/V_2.

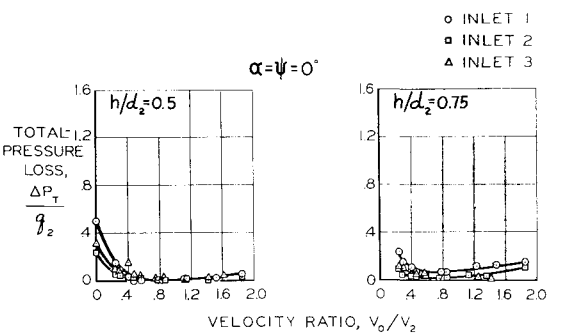

Fig. 10 Effect of engine location on total-pressure loss, lip 1 (scoop vanes closed).

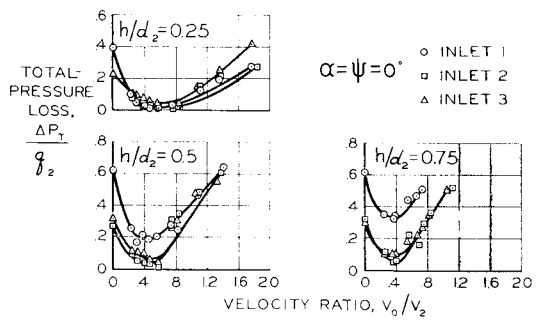

Fig. 11 Effect of engine location on total-pressure loss, lip 2 (scoop vanes closed).

gradients in static and total pressures combine to impose distorted velocity profiles across the compressor blades that can result in blade stall or engine flame-out. Velocity distributions at the engine face were calculated from the measured pressures and the incompressible flow relation $V_L/V_2 = (q_L/q_2)^{1/2}$. Results with and without a scoop are compared in Fig. 9 for conditions descriptive of takeoff and engine restart.

The velocity profiles indicate that performance would be essentially the same at takeoff ($V_0/V_2 = 0$). At restart, when $V_0/V_2 = 1.8$, the basic pod inlet flow has separated from the upstream lip surface, thereby creating a "dead air" region. The remainder of the inlet flow has increased in speed to compensate for the reduction in mass flow in the

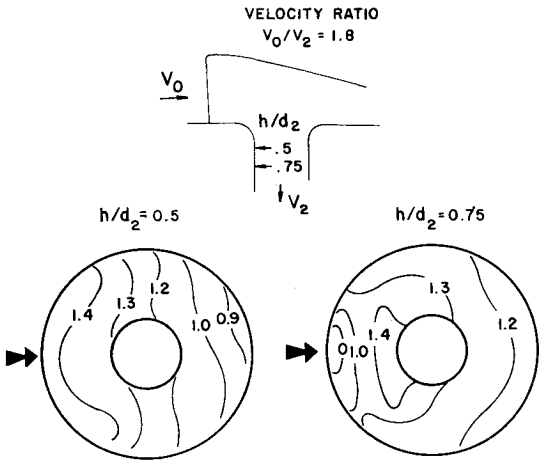

Fig. 12 Effect of engine location on velocity distortion, lip 1; contours are lines of local velocity ratio V_L/V_2.

separated region. In contrast, the scoop-inlet flow is unseparated, and the rapid turning of the flow causes higher velocities forward and lower velocities aft.

The velocity distortion for the scoop inlet at $V_0/V_2 = 1.8$, although less than that for the basic inlet, is still large when compared with distortion at takeoff. However, since restart is not a steady-state flight condition, the distortion could be tolerated if the engine could be accelerated to maximum rpm. It is considered unlikely that the basic inlet could produce acceptable engine accelerations, and even more unlikely that it could produce sufficient ram pressure to windmill the engines to ignition speed. It therefore seems that a scoop inlet is required for acceptable restart performance.

Engine Depth

Velocity distortion at the engine face is caused by gradients in either the static or the total pressure. The static-pressure gradient is caused by flow turning at the inlet and can therefore be reduced by having a long straight section of duct ahead of the engine. On the other hand, the extent of a flow separation increases with distance, and the longer ducts will have greater total-pressure distortion at conditions where separation occurs. Tests were therefore made at various engine depths to establish the duct length for which the combined effects of total- and static-pressure gradients on distortion are minimized.

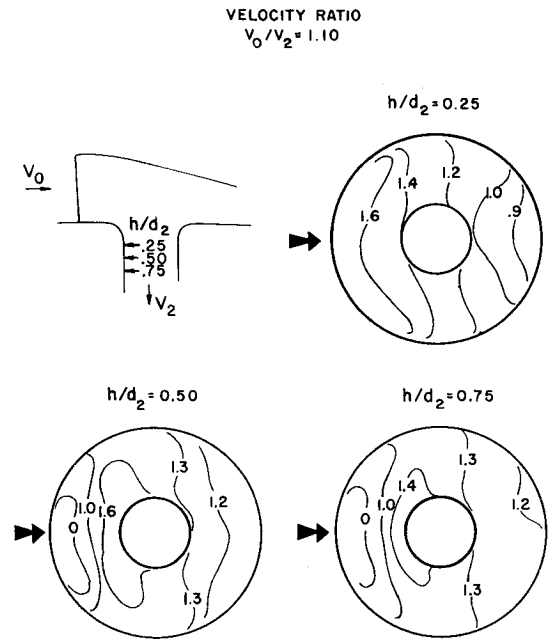

Fig. 13 Effect of engine location on velocity distortion, lip 2; contours are lines of local velocity ratio V_L/V_2.

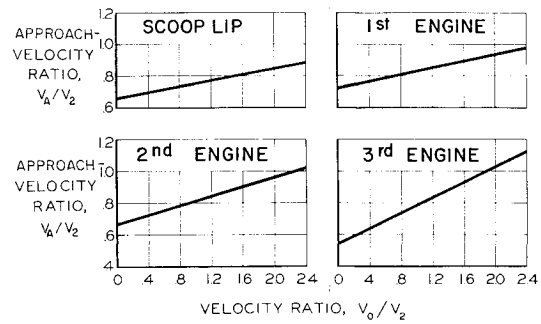

Fig. 14 Calculated scoop internal velocities.

The effect of engine duct length on average total-pressure loss is shown in Figs. 10 and 11. An increase in average loss is shown for both inlet lips as the duct is lengthened. The increase is more pronounced for lip 2, probably because the thinner lip causes a larger separated region. Note that performance for the first inlet of the three deteriorates more rapidly than the performance for the other two. This is probably because of differences in the velocity in the vicinity of each inlet.

The velocity profiles at different engine-face stations for a simulated landing condition are presented in Figs. 12 and 13. The growth of the separated zone is shown at the lower engine locations by the appearance of a region of zero velocity.

It is important to note that the measured gradients are not quite realistic, in that the presence of an engine would affect the pressure gradient on the lip surface and thereby change the flow separation characteristics and the resulting velocity profiles. Further evaluation with an actual engine is needed.

Generalizing Inlet Performance

A prerequisite to designing a distortion generator is an understanding of the nature of the inlet flow. Conditions that cause flow separation and velocity distortion, once known, can be simulated, it is hoped, by a static-test device, thereby facilitating tests with an actual lift engine.

The first step in analyzing the test data is to explain the differences in performance measured with and without a scoop. The analysis of inlet flow based on the concept of lip force (Figs. 1 and 2) indicated that the velocity ratio at the inlet determines the lip force required to turn the flow. This velocity, which will be called the approach velocity (V_A), depends upon the flow area of the scoop. Without the scoop, it is simply the freestream velocity V_0. By comparing data for the scoop- and basic-inlet configurations at the same approach-velocity ratios, some correlation of the data was possible.

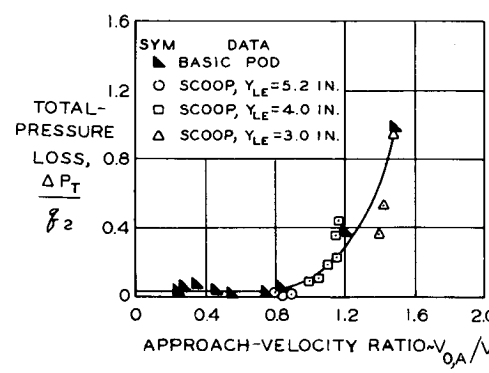

Fig. 15 Inlet performance generalization, lip 1, $h/d_2 = 0.5$.

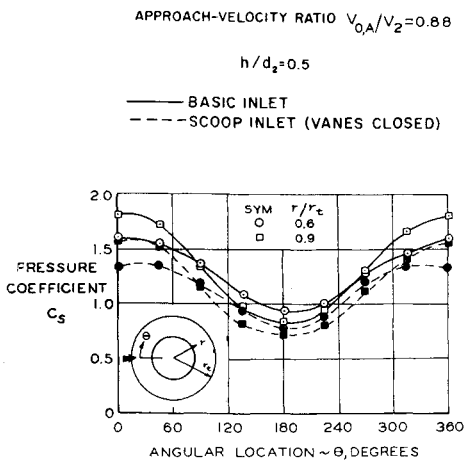

Fig. 16 Comparison of basic- and scoop-inlet static pressures, lip 1.

Accordingly, the scoop approach velocities were calculated by using one-dimensional, incompressible flow relations. The results are presented in Fig. 14 for the scoop configuration discussed earlier. Note that there is a significant effect of velocity ratio V_0/V_2 on the approach velocities. The reason is that the mass flow at the scoop trailing edge becomes an increasingly larger percent of the total mass flow as V_0/V_2 is increased. Minimum trailing-edge height therefore provides maximum diffusion of the oncoming air stream. But since the scoop internal boundary layer must not be ingested, the trailing-edge height must not be zero. Tests made to establish the minimum trailing-edge height showed $\frac{1}{2}$ in. to be optimum for the three-engine pod, and this height was therefore used for the tests described in this paper.

The total-pressure losses of the scoop inlet could now be compared with the pressure losses of the basic inlet. There is an additional loss unaccounted for by this procedure, that is, the pressure loss at the scoop lip caused by flow separation. However, since this loss was eliminated by opening the scoop vanes, the comparison of scoop- and basic-inlet data was made at velocity ratios where lip loss does not occur. Accordingly, the measured scoop-inlet pressure losses are shown in Fig. 15 as a function of the calculated approach-velocity ratios for the various scoop geometries tested. Also shown are the corresponding test results for the basic inlet. Note

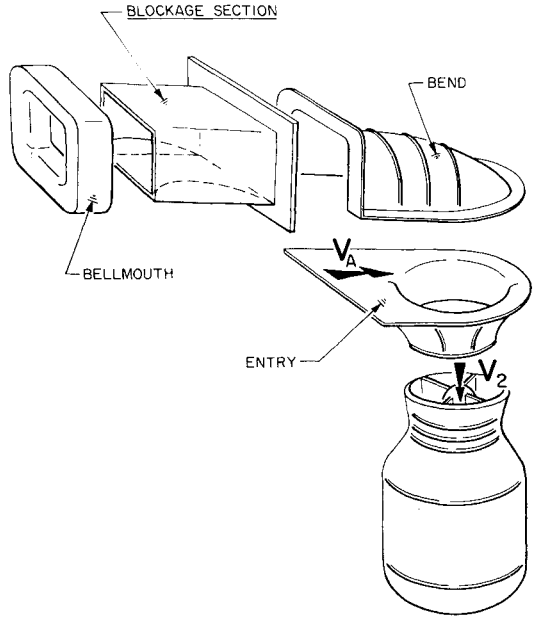

Fig. 17 Distortion generator.

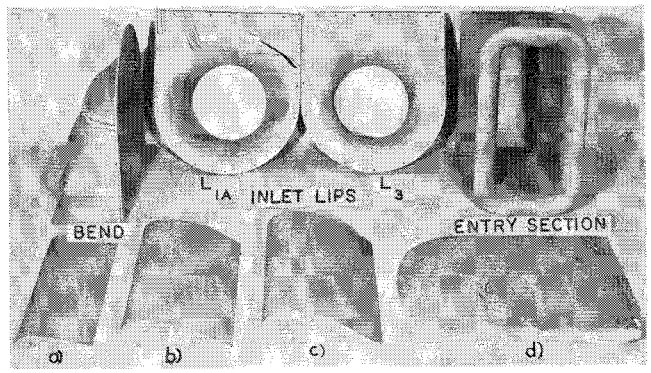

Fig. 18 Distortion generators.

that the basic-inlet data generally agree with scoop performance, indicating that the approach-velocity ratio is a suitable parameter to generalize inlet performance. Further evidence of agreement is shown in Fig. 16 by a comparison of the circumferential static-pressure distribution at the engine. The static pressures were referred to freestream total pressure; hence C_s is, in effect, a dynamic-pressure ratio. Data obtained with the scoop fairing agree reasonably well with data for the basic inlet. The agreement is, in fact, somewhat better than might be expected, in view of the simplicity of the approach-velocity concept used to correlate the data.

Designing a Distortion Generator

The correlation described indicates that the approach-velocity ratio determines inlet performance. This suggests that a device could be built for static tests with a prototype lift engine to duplicate the velocity ratio at the engine entry and thereby simulate in-flight distortions. One possible design for doing this is shown in Fig. 17. The device consists of three sections: a bellmouth entry, a straight section, and a bend that turns the flow into the inlet. The area in the straight section, which determines the approach velocity, can be varied with blockage plates. The bend section approximates the shape of the in-flight streamtube boundary and contributes to the static-pressure gradients at the engine.

This design concept was used in constructing the model components shown in Fig. 18. The airfoil-shaped parts, labeled distortion generators A, B, and C, are blockage plates that can be used either alone or in combination with plate D to give six velocity ratios.

Two lip shapes were tested: lip 1A and lip 3. Lip 1A was the same shape as lip 1 of the wind-tunnel test; lip 3 was nonsymmetrical and had a 5-in. leading-edge radius and a

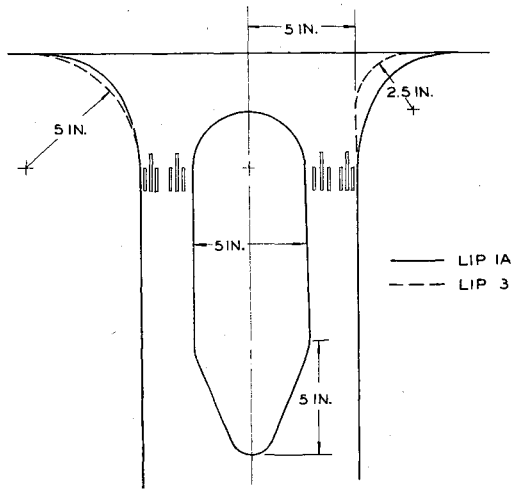

Fig. 19 Distortion-generator inlet.

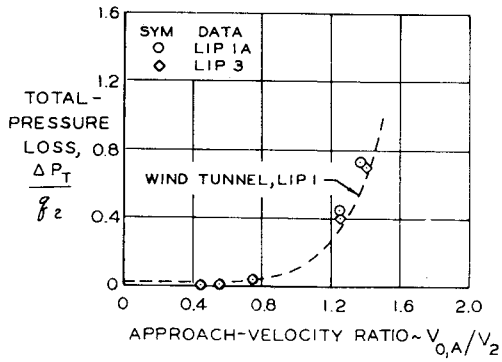

Fig. 20 Comparison of generator and wind-tunnel total-pressure loss, $h/d_2 = 0.5$.

2.5-in. trailing-edge radius. A diagram is presented in Fig. 19 to illustrate the lip shapes and engine-face pressure instrumentation. The pressure rake had the same relative probe locations as the wind-tunnel model.

Generator Pressure Data

Total-Pressure Loss

The distortion generator was connected to the wind-tunnel suction system and tested at an engine-face Mach number of about 0.5. The total-pressure losses measured with blockage plates installed are compared in Fig. 20 with wind-tunnel data for the basic inlet. The velocity approaching the engine entry is based on the minimum flow area in the blockage section. Results for the two lip shapes are very similar and are in good agreement with the wind-tunnel data. Only the data for lip 1*A* are discussed.

Static-Pressure Gradient

The static-pressure gradients at the engine face are primarily caused by the upstream flow turning. Since the streamtube shape is a function of velocity ratio, the use of a fixed-geometry bend imposes some limitation on the ability of the generator to simulate these gradients. However, the trends are in good agreement with the wind-tunnel data, as is shown in Fig. 21. (At $V_A/V_2 = 1.38$, comparison is made with the basic inlet, because velocities inside a properly designed scoop should not reach this high a value.) The high values of C_s between 0° and 80° and between 280° and 360°

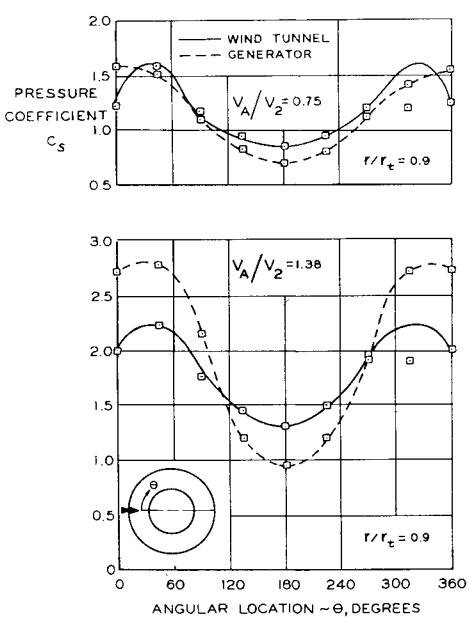

Fig. 21 Comparison of static pressures, lip 1, $h/d_2 = 0.5$.

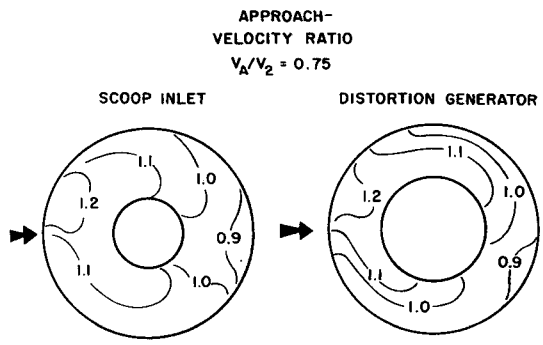

Fig. 22 Comparison of scoop-inlet and generator velocity profiles; contours are lines of local velocity ratio V_L/V_2.

are indicative of the speed increase caused by flow turning. The lower values of C_s between 120° and 240° are caused by stagnation-point flow on the rear lip surface.

Velocity Distortion

The velocity profiles at the engine at $V_A/V_2 = 0.75$ are compared with corresponding wind-tunnel data in Fig. 22. This condition is descriptive of scoop performance at full engine power during the start of transition to vertical landing. Other velocity profiles typical of the distortion generator are shown in Fig. 23. The general patterns of the velocity contours are quite similar to those of the wind-tunnel test. The agreement is further evidence that the distortion generator is a useful device for engine development testing.

Future Work

The distortion-generator design has been submitted to Continental Aviation and Engineering Corporation for full-scale testing with their prototype lift engine. The generator and entry lip will be attached to the compressor face flange. The results of this test and, if possible, later correlation with flight-test or full-scale wind-tunnel data should complete the evaluation of the generator technique.

Summary

A test program was conducted to investigate performance of lift-engine inlets and to develop a static-test method of

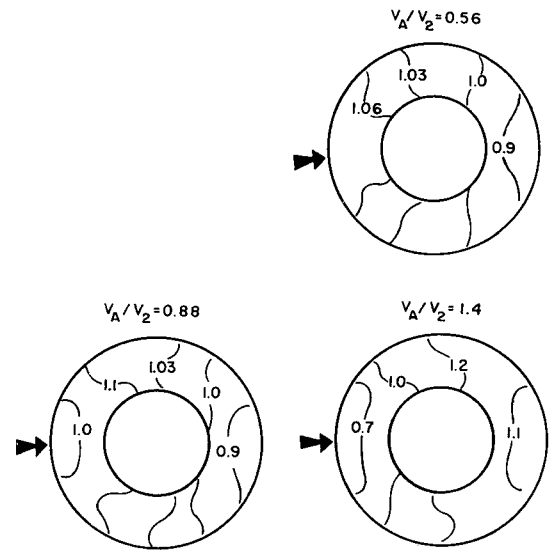

Fig. 23 Generator velocity profiles, lip 1*A*, $h/d_2 = 0.5$; contours are lines of local velocity ratio V_L/V_2.

simulating the flow distortions at the face of a lift engine. Wind-tunnel tests pointed to the combination of high forward speed and low engine power as causing excessive distortion. A scoop inlet was developed that enabled the flow to turn without separation. For improved pressure recovery in static and near-static operation, longitudinal vanes in the top surface of the scoop were used to augment the inlet area. By opening the vanes at low speed and closing them for engine restart, acceptable inlet performance was obtained over the range of flight conditions tested.

The optimum duct length was found to depend upon the influences of static-pressure gradients caused by flow turning and total-pressure gradients caused by flow separation. In general, increasing the duct length improved static-pressure gradients but increased the extent of any flow separation that might have occurred at the entry lip.

The wind-tunnel data showed that, for a given engine-face velocity, the pressure losses, both with and without scoops, were in good agreement when compared at the same approach velocity. This agreement led to the development of a static-test distortion generator that simulated the total- and static-pressure gradients measured in the wind tunnel. The distortion generator had a bellmouth intake and used blockage plates to change the air flow velocity approaching the engine entry. The distortion-generator data agreed well with wind-tunnel data, which indicated that the generator technique should be useful for engine development testing.

Reference

[1] Tyson, B. I., "Tests of air inlets for jet lift engines," Society of Automotive Engineers-American Society of Mechanical Engineers Air Transport and Space Meeting (April 1964).

SEPT.-OCT. 1965 J. AIRCRAFT VOL. 2, NO. 5

Status Report on Liftjets

C. T. HEWSON* AND K. R. DAVIES†
Rolls-Royce, Ltd., Derby, England

A review of 10-yr work on the early RB 108 Liftjet and its derivative, the RB 145, and description of the installation development associated with their respective aircraft are presented in this paper. The lessons learned during this period have proved invaluable to later engine and aircraft designs. The latest Liftjet, the RB 162, which has twice the thrust per unit weight of the early engine, has now been running for two years, and the general design and development are described. The importance of installation from the point of view of installed weight and simplicity of maintenance is discussed. Use of thrust deflection on lift and propulsion jets is possible and has some advantages dependent upon the aircraft reqirements.

I. Experience in VTOL Field

Introduction

WORK at Rolls-Royce on VTOL powerplants and their associated problems has extended over the past ten years. As an introduction to our present and future liftjets, it is interesting to review very briefly these last ten years' work and the lessons learned from this very valuable experience.

We have been involved in several different ways of providing lift thrust for the takeoff of a VTOL aircraft. The Rolls-Royce Avon Engine in the Ryan Verti-Jet provided vertical thrust with the aircraft sitting on its tail. The SC 1 and the Balzac have batteries of pure lift engines to provide all the necessary lift thrust, the propulsion engine being used only for horizontal flight. In between these two extremes comes the deflected propulsive engine thrust for takeoff, which we have achieved by tilting the engine pods as on the German VJ101C, or deflecting the thrust of fixed propulsive engines by means of thrust diverters.

We are actively engaged in reviewing the various methods of thrust deflection in conjunction with several aircraft companies, evolving optimum installations for different aircraft duties.

RB 108 and SC 1 Aircraft

However, by far the major part of our VTOL experience to date has been based on our first design of specialized lifting engine, the RB 108. After a demonstration in 1953 by the "flying bedstead" that a jet-borne vehicle can be stabilized by air jets, the development of the RB 108 was started. Figure 1 is a picture of the "bedstead" during its hover trials.

The RB 108 lift engine, shown in Fig. 2, is a small pure jet engine of low pressure ratio, giving 2200 lb thrust at a thrust weight ratio of 8:1. The engine was designed to power the Short and Harland research aircraft, the SC 1. Four engines provide the lift thrust with high-pressure air bled from each engine compressor to provide aircraft control in roll, pitch, and yaw. The development of the RB 108 installation in the SC 1 has taught us a great deal about the general problems of a pure lift VTO powerplant.

After developing the four-engine system to a satisfactory standard on the test bed, the next big problem that had to be

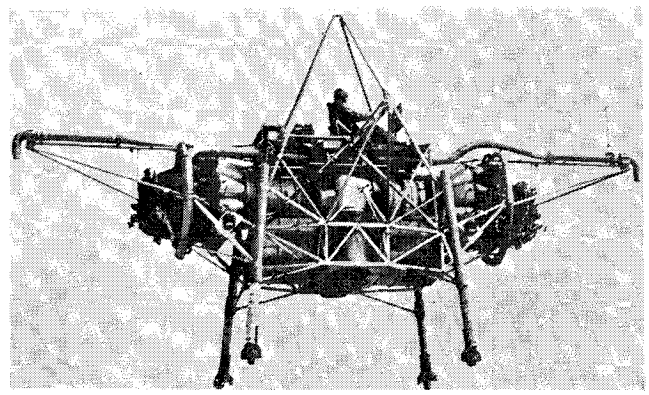

Fig. 1 The flying bedstead.

Presented as Preprint 64-609 at the AIAA Transport Aircraft Design and Operations Meeting, Seattle, Wash., August 10–12, 1964; revision received February 9, 1965.

* Assistant Chief Engineer, Projects.
† Assistant Chief Engineer, Military Engines.